

Catalytic characterization of bi-functional catalysts derived from Pd–Mg–Al layered double hydroxides

N N DAS* and S C SRIVASTAVA

Analytical Chemistry Division, National Metallurgical Laboratory, Jamshedpur 831 007, India

MS received 6 May 2002; revised 17 June 2002

Abstract. Hydrotalcite like precursors containing Pd^{II}–Mg^{II}–Al^{III} with varying molar ratios, (Pd + Mg)/Al ≈ 3 and Mg/Pd ≈ 750 to 35, were prepared by coprecipitation of metal nitrates at constant pH. Characterization of samples as synthesized and their calcined products by elemental analyses, powder XRD, TG–DTA, FT–IR spectroscopy, TPR and N₂ physisorption indicated a well crystalline hydrotalcite like structure with incorporation of Pd²⁺ in the brucite layers. Thermal decomposition of hydrotalcite precursors at intermediate temperatures led to amorphous mixed oxides, Pd/MgAl(O), which on reduction yielded bi-functional catalyst, Pd⁰/MgAl(O). The resultant catalysts with acid, base and hydrogenating sites, were highly active and selective for one-step synthesis of methyl isobutyl ketone (MIBK) from acetone and hydrogen. The results showed an optimal balance between acid-base and metallic sites were required to increase the selectivity of MIBK and stability of the catalysts.

Keywords. Hydrotalcite; palladium; bifunctional catalyst; acetone conversion; MIBK.

1. Introduction

Palladium based catalysts find widespread applications in large varieties of hydrogenation and oxidation reactions (Hickman and Schmidt 1992; Bharadwaj and Schmidt 1995; Lyubovsky and Pfefferle 1999; Sales *et al* 1999; Hill *et al* 2000). Usually, they are prepared by impregnation on various supports to achieve maximum exposure of active component available for the reaction. Although this method ensures the maximum utilization of Pd, the homogeneity and reproducibility of the preparation method may be poor. For a catalytic system, whose activity results from a cooperative effect between active phase and mixed oxide support, a precursor containing all the components homogeneously distributed in the same phase may be a suitable choice. A class of compounds which could be successfully employed as precursors are layered double hydroxides (LDHs) with general formula $[M_{1-x}^{2+}M_x^{3+}(\text{OH})_2]^{x+} \cdot A_{x/n}^{n-} \cdot m\text{H}_2\text{O}$; the widely varied bivalent (Mg, Ni, Co, Zn, Pd etc) and trivalent (Al, Cr, Fe, V etc) metal cations are homogeneously distributed inside the brucite sheets of the layer structure, which on calcination and reduction results in well dispersed, small and stable metal particles on mixed oxide support (Cavani *et al* 1991; Basilea *et al* 1996, 2000, 2001; Narayana and Krishna 1997; Labajos *et al* 1999; Ribet *et al* 1999). A number of Ni, Cu and Co based catalysts (Dung *et al*

1998; Auer *et al* 1999; Velu *et al* 1999a; Coq *et al* 2000) have already been prepared using their corresponding LDH precursors.

Keeping these in view, we have undertaken studies on the preparation of a series of Pd containing MgAl–LDHs and their activation to MgAl(O) mixed oxides by calcination and then reduction to Pd⁰/MgAl(O) bi-functional catalysts. The activity of Pd⁰/MgAl(O), derived from the LDH precursors, have been tested for industrially important one-step synthesis of methylisobutyl ketone (MIBK) from the reaction of acetone and hydrogen, which requires acid-base (for condensation) and metallic (for hydrogenation) functions. It may be noted that several catalytic systems containing Pd, supported on various acid-base supports (Yang and Wu 2000; Das *et al* 2001) have also been tested for this reaction, which showed great influences of acido-basicity and Pd content on the selectivity to MIBK.

2. Experimental

2.1 Preparation of LDH precursors

The LDH precursors with varying Pd/(Mg + Al) were prepared by coprecipitation under low supersaturating condition. A solution containing the metal nitrates in appropriate ratio was slowly added (1 ml/min) to a well-stirred solution of Na₂CO₃ at pH = 9. The pH of the resulting solution was maintained at 9 ± 0.2 by controlled addition of NaOH (1 M) using a pH Stat (718, Titrimo,

*Author for correspondence

Metrohm). Once the addition was completed, the resulting slurry was digested at 80°C for 15 h. The precipitate was separated by centrifugation, washed with distilled water until the washings were free from nitrate and dried overnight in air at 80°C.

The nitrate ions from the interlayer were replaced by carbonate by suspending the nitrate precursors (2 g) in a solution of Na₂CO₃ (0.2 M, 100 ml) and stirring for 2 h. This was repeated twice after replacing the Na₂CO₃ solution with a fresh one to ensure complete removal of nitrate. The carbonate-exchanged solid was dried overnight at 80°C.

2.2 Characterization

Elemental analyses of the carbonate-exchanged samples were done by ICP-MS. The powder X-ray diffractions were recorded on a CGR Theta 60 diffractometer equipped with a nickel filtered CuK_α radiation (35 kV, 15 mA). The crystalline phases were identified by comparison with JCPDS data base and previously reported data. Thermogravimetric analyses, in the range 20–850°C, were carried out on a SETARAM TG 85 microbalance under a flow of air (80 ml/min) and a heating rate of 5°C/min. FT-IR in KBr phase were recorded in a Nicolet Spectrometer with a nominal resolution of 2 cm⁻¹ and averaging 100 scans to improve signal to noise ratio. The nitrogen adsorption-desorption isotherms for specific surface area and porosity assessment were recorded at -193°C using ASAP 2010 from Micromeritics after degassing the sample under vacuum (2 × 10⁻⁴ Pa) at 250°C overnight.

Temperature programmed reduction (TPR) of the calcined samples were performed in a Autochem 2910 from Micromeritics, using a 3% H₂/Ar (v/v) mixture as reducing agent to know the reduction behaviour of the materials. The experimental conditions such as amount of sample, heating rate, H₂/Ar flow were chosen according to the data reported elsewhere (Reiche *et al* 2000), in order to reach good resolution of the reduction peaks. Hydrogen chemisorption were carried out by the pulse technique using the same instrument. After reactivation at 200°C with H₂ for 4 h, the sample was cooled in air then maintained at 50 ± 0.1°C. Pulses of 500 μL of H₂/Ar (3/97, Ultra high purity gas) were fed to the sample till completion of the chemisorption. 10 minutes of equilibrium was allowed after each pulse.

2.3 Calcination and activation of samples

The carbonate exchange samples were calcined in air (flow 100 ml/min) at the desired temperature (5°C/min) for 5 h. The calcined products were reduced in diluted hydrogen (H₂/N₂ = 10/90, flow: 60 ml/min) at different temperatures (ramp: 2°C/min) for 5 h.

2.4 Catalytic test

The catalytic activity was performed under atmospheric pressure in a micro-flow fixed bed reactor (6 m i.d.) using 50–100 mg catalysts. Prior to any measurement, the catalysts were subjected to *in situ* activation in H₂ at 200°C for 2 h (ramp: 2°C/min). Acetone was fed by bubbling H₂/He mixture through a saturator at 0°C ($P_{\text{acetone}} = 8.4$ kPa). The reaction mixture was then passed through the catalyst and the effluent drawn at regular time intervals was analysed by an on line gas chromatograph (Carlo-Erba) equipped with a capillary column (30 m × 0.53 mm i.d. Carbowax 20 M bonded phase) and a flame ionization detector. All the connecting lines, commutation and sampling valves were placed in a box heated at 120°C in order to prevent any condensation. The following parameters were determined to evaluate the catalytic properties.

$$\text{Acetone conversion (mol\%)} = 100 \times \frac{\text{acetone}_{\text{in}} - \text{acetone}_{\text{out}}}{\text{acetone}_{\text{in}}}$$

$$\text{Selectivity in product (mol\%)} = 100 \times \frac{\text{Corrected area}}{\text{Sum of all corrected areas of products}}$$

The selectivity has been calculated from peak areas taking response factor of different products in the flame ionization detector into account. In the course of reaction of acetone and hydrogen, we detected propane-2-ol (IPA), 4-methyl-2-pentanone (MIBK), 2,6-dimethyl-4-heptanone (DIBK) as main products and 4-methyl-3-pentene-2-one (MO), 3,5,5-trimethyl-2-cyclohexene-1-one (IPHO), 3,3,5-trimethylcyclohexanone (TMCO), 4-methyl-pentane-2-ol (MIBA) and 2,6,8-trimethylnonan-4-one (C₉) as secondary products. The nature of the products was determined by comparing the retention times with standard samples and also by GC-MS coupling.

3. Results and discussion

3.1 Chemical compositions

The chemical compositions of the carbonate exchange samples, derived from elemental analyses for Pd, Mg, Al, C and N contents and from thermogravimetric measurements for amount of structural water, are summarized in table 1. The nitrogen content is always found to be < 0.2 wt% and therefore, not taken into account for calculation of molecular formulae of LDHs. The molar composition of Pd and Al are always close to the composition of the original solution while that of Mg is always slightly lower than expected as the coprecipitation carried out at pH ≈ 9. The excess of anionic charge

Table 1. Chemical composition and lattice parameters of HT precursors.

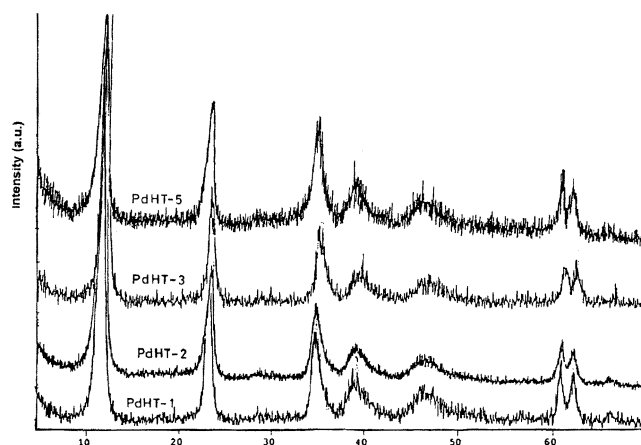
Sample	Mg/Pd	Chemical compositions	<i>a</i> (nm)	<i>c</i> (nm)
PdHT-1	766	[Pd _{0.0076} Mg _{5.82} Al _{2.17} (OH) ₁₆](CO ₃) _{1.18} ·5·12H ₂ O	0.3052	2.296
PdHT-2	348	[Pd _{0.0167} Mg _{5.81} Al _{2.18} (OH) ₁₆](CO ₃) _{1.11} ·5·60H ₂ O	0.3055	2.312
PdHT-3	129	[Pd _{0.045} Mg _{5.79} Al _{2.16} (OH) ₁₆](CO ₃) _{1.14} ·5·44H ₂ O	0.3049	2.312
PdHT-4	59	[Pd _{0.095} Mg _{5.62} Al _{2.28} (OH) ₁₆](CO ₃) _{1.18} ·5·18H ₂ O	0.3051	2.263
PdHT-5	37	[Pd _{0.153} Mg _{5.67} Al _{2.18} (OH) ₁₆](CO ₃) _{1.10} ·5·28H ₂ O	0.3053	2.315

observed in some samples could be accounted for by the presence of bi-carbonate or neutral carbonate species weakly bonded to the surface of the crystal (Del Arco *et al* 1996). The water content in the interlayer is well within the expected values for this sort of materials; the maximum number of water molecules in interlayer per formula of hydrotalcite like materials, $[M_{1-x}^{2+}M_x^{3+}(\text{OH})_2](\text{CO}_3)_{x/2} \cdot n\text{H}_2\text{O}$ would be $n \leq 2 - 3x/2$ (Miyata 1993).

3.2 X-ray diffractions

Powder XRD diffraction pattern for carbonate exchange samples dried at 80°C (see figure 1) showed sharp and symmetrical reflections for (003), (006), (110), (113) planes and broad asymmetrical peaks for (012), (015), (018) planes. All these peaks are characteristics of well crystalline single hydrotalcite like phase (LDH: JCPDS File no. 38-487) (Reichle *et al* 1986; Weir *et al* 1997). This also indicates that Pd²⁺ ion is isomorphously substituted for Mg in the Mg–Al brucite layer, although it favours the formation of square planer coordinated compounds (Greenwood and Earnshaw 1989) and has comparatively higher ionic radius (0.086 nm). It has been reported that several bivalent metal ions with comparable ionic radii, e.g. Ni²⁺ (0.083 nm), Pt²⁺ (0.081 nm), Zn²⁺ (0.074 nm) etc, isomorphously substituted for Mg²⁺ leading to well crystalline single phase hydrotalcite like compounds (Weir and Kydd 1988; Dung *et al* 1998; Ennadi *et al* 2000; Basilea *et al* 2001). Assuming a hexagonal structure, the lattice parameters '*a*' and '*c*' of the LDH phase were calculated from (110) and (003) reflections and reported in table 1. These values compare well with those reported for MgAl–LDH (Cavani *et al* 1991). The variation, however, is too small to draw any finite conclusions.

Powder XRD patterns of PdHT-5, calcined at ≥ 400°C, showed (see figure 2) the characteristic peaks of a poorly crystalline MgO like phase due to collapse of layered structure. The lattice constant '*a*' is always slightly smaller than that of pure MgO, indicating incorporation of Al³⁺ in the lattice as also reported previously by several workers (Cavani *et al* 1991; Rebours *et al* 1994; Vaccari 1999). As the Pd contents in the samples are relatively small and overlapping of peaks of PdO on MgO (Basilea *et al* 2000), no characteristic peak for PdO could be detected in the calcined samples.

**Figure 1.** Powder XRD patterns of uncalcined Pd containing MgAl–LDHs.

3.3 TG–DTA analysis

The decomposition of a selected carbonate exchanged sample in air, followed by thermogravimetric analysis between 20 and 800°C, is presented in figure 3. All the samples exhibit weight losses in two consecutive endothermic stages; the total weight losses vary in the range 42–45%. The first weight loss is ascribed to removal of molecular water from the interlayer space while the second one corresponds to evaluation of CO₂ from interlayer carbonate and water vapours through condensation of hydroxyl groups in the brucite layers. These behaviours are in agreement with those reported for LDHs (Hibino *et al* 1995; Bellotto *et al* 1996). Further evidence is obtained from analysis of evolved gases during decomposition for masses: 18(H₂O), 30(NO), 44(CO₂), 46(NO₂) (see figure 3, inset). Only a trace amount of NO₂ (mass 46) is detected indicating the exchange is not 100% as also obtained in chemical analysis.

3.4 FT–IR spectra

The FT–IR spectra of a selected sample and that calcined at 400°C are shown in figure 4. A broad absorption band at 3450 cm⁻¹ is attributed to stretching of hydrogen bonded hydroxyl group and water molecules; the corresponding deformation mode (*d*_{H₂O}) appeared at ~ 1630 cm⁻¹

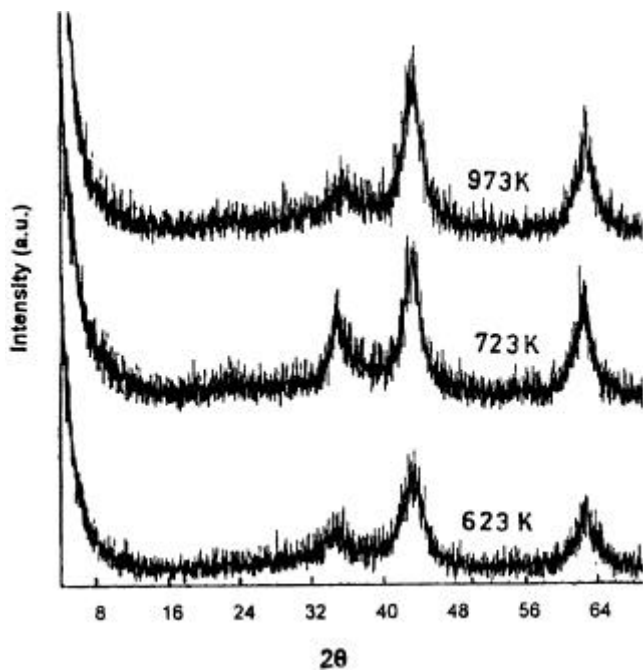


Figure 2. Powder XRD patterns of Pd containing MgAl-LDH (PdHT-5) calcined at 450°C.

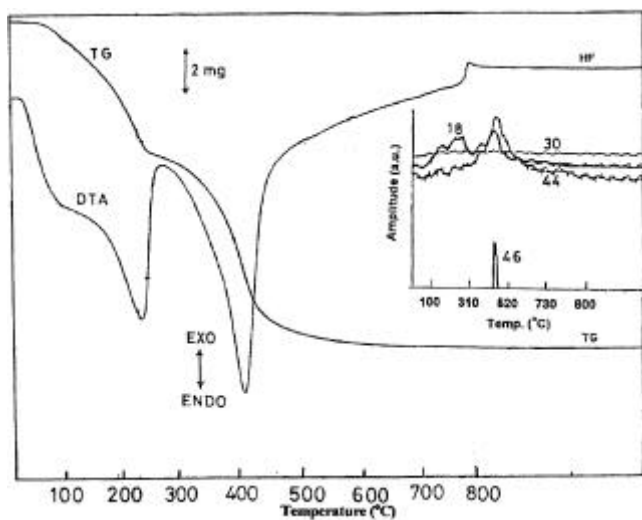


Figure 3. TG-DTA and mass spectroscopic (inset) analyses of evolved gas during decomposition of PdHT-2.

(Cavani *et al* 1991; Velu *et al* 1999b). The presence of a weak shoulder at $\sim 3200\text{ cm}^{-1}$, causing the broadness of this band, is ascribed to the OH stretching mode of water molecules hydrogen bonded to CO_3^{2-} ions. The absorption bands n_3 , n_2 and n_4 due to stretching vibration of inter-layer CO_3^{2-} ions (Cavani *et al* 1991; Velu *et al* 1999b) were observed at ~ 1380 , 823 and 662 cm^{-1} , respectively. It is worthwhile to note that if the carbonate ion lies in a site of lower symmetry (e.g. C_{2v}) than the unperturbed carbonate (i.e. D_{3h}), the band observed at $\sim 1380\text{ cm}^{-1}$ would resolve into two lines due to removal of dege-

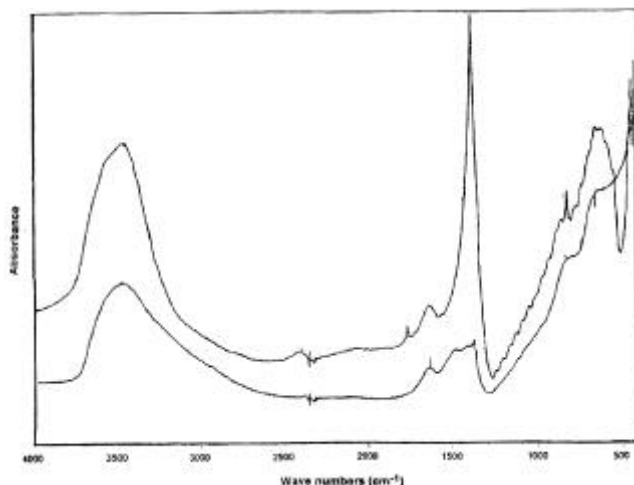


Figure 4. FT-IR spectra of PdHT-2 (a) uncalcined and (b) calcined at 450°C.

Table 2. Specific surface areas and average pore diameter of samples calcined at 450°C.

Sample	Surface area (m^2/g)	Avg. pore diameter (\AA)	Pore volumes (cm^3/g)
PdHT-1	231	64.9	0.32
PdHT-2	254	48.6	0.38
PdHT-3	237	52.7	0.32
PdHT-4	260	45.6	0.43
PdHT-5	227	63.3	0.30

neracy of the n_3 mode. In addition, the n_1 vibration at $\sim 1050\text{ cm}^{-1}$ will become IR active. Neither any splitting of n_3 mode nor absorption band corresponds to n_1 mode were found, indicating the CO_3^{2-} ion lies in a symmetrical site between two adjacent brucite layers in parallel direction (Cavani *et al* 1991; Aramendia *et al* 1999). On calcination at 450°C, the intensities of all bands are greatly reduced. The presence of broadened absorption band at $\sim 3450\text{ cm}^{-1}$ indicated that a sizeable amount of hydroxyl groups are still present in the brucite layer. Also, the absorption band due to n_3 mode splits into two lines indicating the symmetric feature of CO_3^{2-} site was lost in the calcined sample.

3.5 Textural analysis

The uncalcined samples have low specific surface areas ($\sim 40\text{ m}^2/\text{g}$), which upon calcination at 450°C increases up to $260\text{ m}^2/\text{g}$ (see table 2), owing to formation of pores due to H_2O and CO_2 venting. All the samples exhibit type-IV isotherms of IUPAC classification (Sing *et al* 1985) due to capillary condensation in mesopores where adsorption is limited for high relative pressure. The hysteresis loops (H2 type) are characteristic of pores with

narrow necks. The mean pore diameters of the calcined sample vary in the range 45–65 Å (table 2).

3.6 Reduction of mixed oxides

The ease by which Pd reduced is assessed by temperature programmed reduction of the mixed oxides. TPR profile of a selected mixed oxide derived from PdHT-5 is presented in figure 5. The intense positive peak in the range 150–450°C is due to reduction of Pd²⁺ or PdO to Pd. This reduction of temperature is much higher than that of PdO alone indicating a strong interaction between PdO and MgAl(O) which inhibits the reduction (Binet *et al* 1992; Chen *et al* 1998). As expected the position of the reduction peak shifted to lower temperature and became narrow with increasing Pd content. A small negative peak centred at ~60°C, invariably observed in all samples, was attributed to the Pd-*b* hydride decomposition (Lietz *et al* 1998), which results from the reduction of trace amount of Pd at room temperature (Zhang *et al* 1992). The total consumption of hydrogen for reduction of PdO to Pd⁰, expressed as H₂/Pd, is always found to be slightly more than unity. The excess hydrogen uptake is presumably due to reduction of trace amount of NO₃⁻ ion present in the calcined samples which is also evident

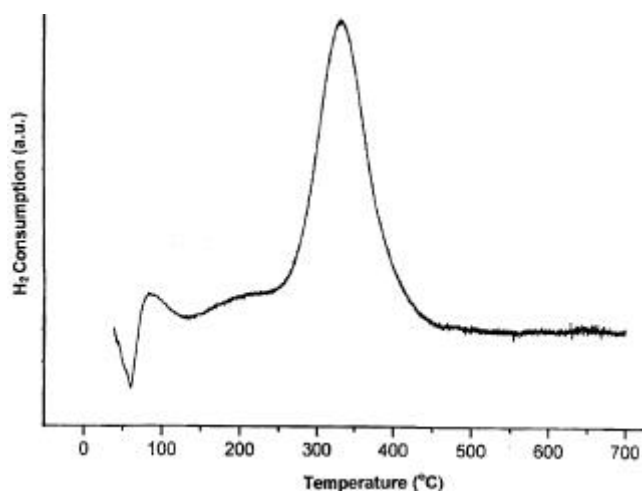


Figure 5. Temperature reduction profile of PdHT-5 calcined at 450°C.

Table 3. Dispersion and average particle size of Pd in Pd⁰/MgAl(O).

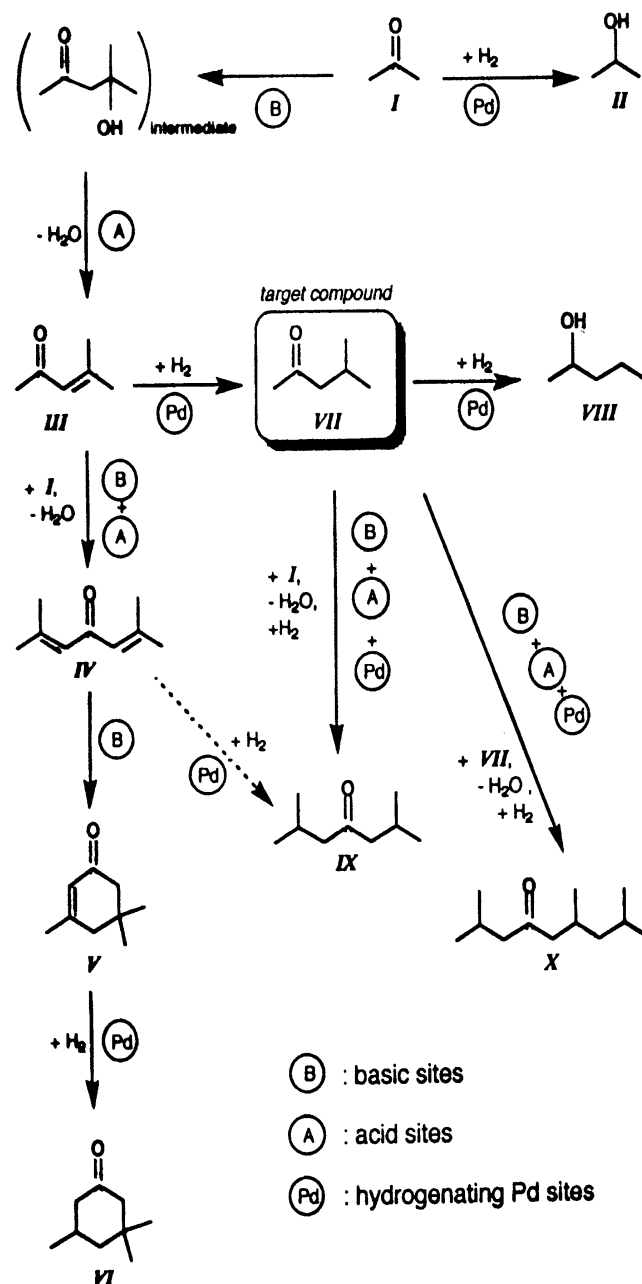
Sample	Pd (wt.%) ^a	Dispersion (%)	Av. particle size (nm)
PdHT-1	0.22	16.2	6.2
PdHT-2	0.48	12.8	7.8
PdHT-3	1.28	11.2	8.9
PdHT-4	2.80	8.5	11.8
PdHT-5	4.58	4.9	20.5

^aWt.% of Pd in samples calcined at 450°C.

from chemical and TG-MS analyses. As expected, the accessibility of Pd, derived from the uptakes of irreversibly adsorbed hydrogen ($D = Pd_{\text{surf}}/Pd_{\text{tot}} \approx H/Pd$) and assuming a chemisorption stoichiometry of $H_{\text{ad}}/P_{\text{ds}} = 1$, decreases with increase of Pd content in the mixed oxide (see table 3). The average particle size, calculated from an empirical relationship $d_p(\text{nm}) = 1/D$, are ≤ 20 nm.

3.7 Catalytic tests

In one-step synthesis of MIBK from acetone, using Pd based catalysts (Yang and Wu 2000; Das *et al* 2001), a



Reaction Scheme I.

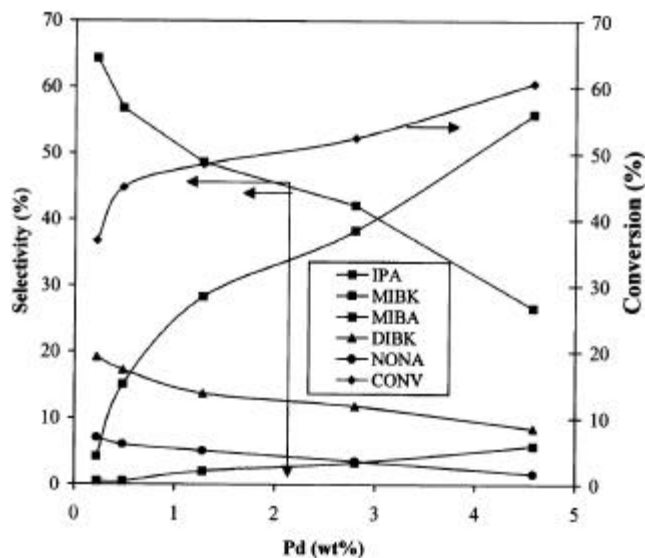


Figure 6. Acetone conversion and products selectivity over various Pd⁰/MgAl(O) derived from Pd containing MgAl-LDHs.

number of side reactions take place simultaneously (see reaction scheme-I). Besides aldol condensation of acetone to form diacetone alcohol (DAA), it can be hydrogenated to IPA. DAA dehydrated to mesityl oxide (MO) which further undergo condensation and/or hydrogenation to form IPHO and TMCO or MIBK, respectively. MIBK may further proceed aldol condensation and/or hydrogenation to form DIBK or MIBA, respectively. Self-condensation of MIBK followed by hydrogenation may yield C₉+ products. In order to obtain high yield of MIBK, the reaction temperature, a balance between metallic and acid-base sites, the acetone/H₂ ratio etc are of paramount importance (Yang and Wu 2000; Das *et al* 2001).

The preliminary results on catalytic activity of Pd⁰/MgAl(O) for one-step synthesis of MIBK from acetone, under best experimental conditions derived in our previous study (Das *et al* 2001), are summarized as follows. The distribution of various products with respect to Pd contents is depicted in figure 6. Although the conversion of acetone increased with increase in Pd loading, MIBK selectivity decreased markedly because Pd might aggregate and cover some of the basic sites. The high hydrogenation activities of catalysts with high Pd content favours the hydrogenation of >C=O of acetone to IPA in the competition between hydrogenation and the condensation reactions. The MIBK selectivity increased up to 75% at lower Pd loading (Pd ~ 0.2 wt%) mainly at the expense of IPA. The catalyst (derived from PdHT-1), however, deactivated with time and the conversion of acetone decayed from 36 to merely 9% in 6 h.

Further studies are needed to optimize a balance between the metallic and acid-base functions to increase the MIBK selectivity and stability of the catalysts.

4. Conclusions

Ternary hydrotalcite like precursors containing Pd, Mg and Al in the brucite layers were prepared by coprecipitation at constant pH. Calcination of precursors at intermediate temperature lead to formation of amorphous mixed oxides, which on reduction at 200°C yield Pd⁰/MgAl(O) with average Pd particle size ranging from 6–20 nm. Higher reduction temperature for Pd in Pd/MgAl(O) compared to PdO alone indicate a strong interaction between Pd and MgAl(O). Pd⁰/MgAl(O) catalysts with acid, base and hydrogenating properties are active and selective, at least at low Pd content, in the one-step synthesis of MIBK from acetone and hydrogen. The selectivity to MIBK can be improved further by means of an optimal balance between metallic and acid-base sites.

Acknowledgement

One of the authors (ND) is thankful to Dr D Tichit, Laboratoire de Materiaux Catalytiques et Catalyses en Chimie Organique, UMR 5618 CNRS, Montpellier, France for providing laboratory facilities and many helpful discussions during his stay in France as a BOYSCAST Fellow.

References

- Aramendia M A, Aviles Y, Benitez J A, Borau V, Jimenez C, Marinas J M, Ruiz J R and Urbano J 1999 *Microporous and Mesoporous Mater.* **29** 319
- Auer S M, Gredig S V, Koppel R A and Baiker A 1999 *J. Mol. Catal. A* **141** 193
- Basilea F, Basini L, Fornasari G, Gazzanob M, Trifiro F and Vaccari A 1996 *J. Chem. Soc. Chem. Commun.* 2435
- Basilea F, Gazzanob M, Trifiro F and Vaccari A 2000 *Appl. Clay Sci.* **16** 185
- Basilea F, Fornasari G, Gazzanob M, Trifiro F and Vaccari A 2001 *Appl. Clay Sci.* **18** 51
- Bellotto M, Rebours B, Clause O, Lynch J and Elkaim E 1996 *J. Phys. Chem.* **100** 8535
- Bharadwaj S S and Schmidt L D 1995 *Fuel Process Technol.* **42** 109
- Binet C, Jodi A, Lavalley J C and Boutonnet-Kizing M 1992 *J. Chem. Soc., Faraday Trans.* **88** 2079
- Cavani F, Trifiro F and Vaccari A 1991 *Catal. Today* **11** 173
- Chen Y Z, Hwang C M and Lian C W 1998 *Appl. Catal.* **169** 207
- Coq B, Tichit D and Ribet S 2000 *J. Catal.* **189** 117 and references therein
- Das N N, Tichit D, Durand R, Graffin P and Coq B 2001 *Catal. Lett.* **71** 181 and references therein
- Del Arco M, Rives V, Trujillano R and Malet P 1996 *J. Mater. Chem.* **6** 1419
- Dung N T, Tichit D, Chiche L H and Coq B 1998 *Appl. Catal. A* **169** 179 and references therein

- Ennadi A, Legrouri A, De Roy A and Besse J-P 2000 *J. Mater. Chem.* **10** 2337
- Greenwood N N and Earnshaw A 1989 *Chemistry of elements* (Oxford: Pergamon) p. 125
- Hibino T, Yamashita Y, Kosuge K and Tsunashina K 1995 *Clays Clay Miner.* **43** 427
- Hickman D A and Schmidt L D 1992 *J. Catal.* **138** 267
- Hill J M, Shen J, Watwe R M and Dumesic J A 2000 *Langmuir* **16** 2213
- Labajos F M, Sastre M D, Trujillano R and Rives V 1999 *J. Mater. Chem.* **9** 1033
- Lietz J, Nimz M and Volter J 1998 *Appl. Catal.* **45** 71
- Lyubovsky M and Pfefferle L 1999 *Catal. Today* **47** 29
- Miyata S 1993 *Clays Clay Miner.* **41** 551
- Narayana S and Krishna K 1997 *J. Chem. Soc., Chem. Commun.* 1991
- Rebours R, Caillerie J B and Clause O 1994 *J. Am. Chem. Soc.* **116** 1707
- Reiche M A, Maciejewski M and Baiker A 2000 *Catal. Today* **56** 347
- Reichle W T, Kang S Y and Everhardt D S 1986 *J. Catal.* **101** 352
- Ribet S, Tichit D, Coq B, Ducourant B and Morato F 1999 *J. Solid State Chem.* **142** 1033
- Sales E A, Bughi G, Ensuque A, Mendes M J and Verduraz F B 1999 *Phys. Chem. Chem. Phys.* **1** 491 and references therein
- Sing S K W, Everett D H, Wttaul R A, Moscou L, Pierotti R, Rouquerol J and Sieminiewska T 1985 *Pure and Appl. Chem.* **57** 603
- Vaccari A 1999 *Appl. Clay Sci.* **14** 161
- Velu S, Suzuki K and Osaki T 1999a *Catal. Lett.* **62** 159
- Velu S, Shah M, Jyothi T M and Sivasankar S 1999b *Micro-porous and Mesoporous Mater.* **33** 61
- Weir M R and Kydd R A 1988 *Inorg. Chem.* **37** 5619
- Weir M R, Moore J and Kydd R A 1997 *Chem. Mater.* **9** 1686 and references therein
- Yang S M and Wu M Y 2000 *Appl. Catal. A* **192** 211 and references therein
- Zhang A, Schwarz J A, Datya A and Baltrus J P 1992 *J. Catal.* **138** 55